Maximum mass of neutron stars

H.-J. Schulze
INFN Sezione di Catania, Via Santa Sofia 64, I-95123 Catania, Italy

A. Polls and A. Ramos
Departament ECM, Universitat de Barcelona, Av. Diagonal 647, E-08028 Barcelona, Spain

I. Vidaña
Gesellschaft für Schwerionenforschung (GSI), Planckstrasse 1, D-64291 Darmstadt, Germany
(Received 9 December 2005; published 9 May 2006)

We determine the structure of neutron stars within a Brueckner-Hartree-Fock approach based on realistic nucleon-nucleon, nucleon-hyperon, and hyperon-hyperon interactions. Our results indicate rather low maximum masses below 1.4 solar masses. This feature is insensitive to the nucleonic part of the EOS due to a strong compensation mechanism caused by the appearance of hyperons and represents thus strong evidence for the presence of nonbaryonic "quark" matter in the interior of heavy stars.

DOI: 10.1103/PhysRevC.73.058801 PACS number(s): 26.60.+c, 13.75.Ev, 24.10.Cn, 97.60.Jd

The only way to obtain information on the structure and properties of baryonic matter at extreme densities of several times normal nuclear matter density $\rho_0 \approx 0.17$ fm^{-3} seems to be the theoretical modelling of neutron stars, the unique environment where such densities are actually reached in nature, and the subsequent confrontation with observational data. Any given equation of state (EOS) of baryonic matter determines uniquely the mass-radius relation of neutron star sequences and in particular the maximum mass a neutron star can achieve before collapsing into a black hole.

Most theoretical investigations performed so far point to an important feature of high-density β-stable matter, namely that hyperons will appear at densities of about $2, \ldots, 3$ ρ_0 and strongly soften the EOS. The main consequence is a substantial reduction of the maximum mass [1]. This seems to be an inevitable feature of any approach taking into account the hyperons, caused simply by the availability of additional degrees of freedom of the matter at high density. Any theoretical study of neutron stars without allowing for the presence of hyperons is therefore unrealistic.

Evidently it is then important to carry out microscopic calculations as precisely as possible in order to make reliable predictions for the maximum mass of a neutron star composed of baryonic matter and the eventual confrontation with observational data. In this work we report on recent results following this motivation. We try to present strong evidence that the maximum mass of baryonic neutron stars is very low and that therefore neutron stars with larger masses (above ca. 1.5 solar masses) must necessarily contain quark matter.

Our theoretical framework is the nonrelativistic Brueckner-Hartree-Fock (BHF) approach based on microscopic nucleon-nucleon (*NN*), nucleon-hyperon (*NY*), and hyperon-hyperon (*YY*) potentials that are fitted to scattering phase shifts, where possible. Nucleonic three-body forces (TBF) are included in order to (slighty) shift the saturation point of purely nucleonic matter to the empirical value.

It has been demonstrated that the theoretical basis of the BHF method, the hole-line expansion, is well founded: the nuclear EOS can be calculated with good accuracy in the BHF two hole-line approximation with the continuous choice for the single-particle potential, since the results in this scheme are quite close to the full convergent calculations which include also the three hole-line contribution [2]. Due to these facts, combined with the absence of adjustable parameters, the BHF model is a reliable and well-controlled theoretical approach for the study of dense baryonic matter.

We begin with a short review of the BHF approach including hyperons. Detailed accounts can be found in Refs. [3] and [4]. The basic input quantities in the Bethe-Goldstone equation are the *NN*, *NY*, and *YY* potentials. In our work we use the Argonne V_{18} *NN* potential [5] supplemented by either the semiphenomenological Urbana UIX nucleonic TBF of Ref. [6] or the microscopic GLMM three-body forces of Refs. [7,8], and the Nijmegen soft-core *NY* and *YY* potentials (either NSC89 [9] or the NSC97e model of Ref. [10]) that are well adapted to the existing experimental *NY* scattering data and also compatible with Λ hypernuclear levels [11,12]. Unfortunately, up to date no *YY* scattering data exist and therefore no reliable *YY* potentials are available. Thus the NSC89 potentials contain no *YY* components, whereas the NSC97 potentials comprise extensions to the *YY* sector based on SU(3) symmetry. Nevertheless the importance of *YY* potentials should be minor as long as the hyperonic partial densities remain limited.

With these potentials, the various G matrices are evaluated by solving numerically the Bethe-Goldstone equation, which can be written in operatorial form as

$$G_{ab}[W] = V_{ab} + \sum_c \sum_{p,p'} V_{ac}|pp'\rangle \frac{Q_c}{W - E_c + i\epsilon} \langle pp'|G_{cb}[W], \tag{1}$$

where the indices a, b, c indicate pairs of baryons and the Pauli operator Q and energy E determine the propagation of

intermediate baryon pairs. The pair energy in a given channel $c = (B_1 B_2)$ is

$$E_{(B_1 B_2)} = T_{B_1}(k_{B_1}) + T_{B_2}(k_{B_2}) + U_{B_1}(k_{B_1}) + U_{B_2}(k_{B_2}) \quad (2)$$

with $T_B(k) = m_B + k^2/2m_B$, where the various single-particle potentials are given by

$$U_B(k) = \sum_{B'=n,p,\Lambda,\Sigma^-} U_B^{(B')}(k) \quad (3)$$

and are determined self-consistently from the G matrices,

$$U_B^{(B')}(k) = \sum_{k'<k_F^{(B')}} \mathrm{Re}\langle kk'|G_{(BB')(BB')}[E_{(BB')}(k,k')]|kk'\rangle. \quad (4)$$

The coupled equations (1)–(4) define the BHF scheme with the continuous choice of the single-particle energies. In contrast to the standard purely nucleonic calculation, the additional coupled channel structure renders the calculations quite time-consuming.

Once the different single-particle potentials are known, the total nonrelativistic baryonic energy density, ϵ, can be evaluated:

$$\epsilon = \sum_{B=n,p,\Lambda,\Sigma^-} \sum_{k<k_F^{(B)}} \left[T_B(k) + \frac{1}{2} U_B(k) \right] = \epsilon_N + \epsilon_Y, \quad (5)$$

where

$$\epsilon_N = \sum_{N,N'=n,p} \sum_{k<k_F^{(N)}} \left[T_N(k) + \frac{1}{2} U_N^{(N')}(k) \right], \quad (6)$$

$$\epsilon_Y = \sum_{\substack{Y,Y'=\Lambda,\Sigma^- \\ N=n,p}} \sum_{k<k_F^{(Y)}} \left[T_Y(k) + U_Y^{(N)}(k) + \frac{1}{2} U_Y^{(Y')}(k) \right]. \quad (7)$$

Knowing the baryonic energy density Eq. (5), and adding the contributions of the noninteracting leptons, the various chemical potentials $\mu_i = \partial\epsilon/\partial\rho_i$ (of the species $i = n, p, \Lambda, \Sigma^-, e, \mu$) can be computed straightforwardly and the equations for beta-equilibrium, $\mu_i = b_i\mu_n - q_i\mu_e$, ($b_i$ and q_i denoting baryon number and charge of species i) and charge neutrality, $\sum_i \rho_i q_i = 0$, allow one to determine the equilibrium composition $\rho_i(\rho)$ at given baryon density ρ and finally the EOS,

$$p(\rho) = \rho^2 \frac{d}{d\rho} \frac{\epsilon(\rho_i(\rho))}{\rho} = \rho \frac{d\epsilon}{d\rho} - \epsilon. \quad (8)$$

Knowing the EOS, the equilibrium configurations of static neutron stars are obtained by solving the Tolman-Oppenheimer-Volkoff (TOV) equations [1] for the pressure $p(r)$ and the enclosed mass $m(r)$,

$$\frac{dp}{dr} = -\frac{Gm\epsilon}{r^2} \frac{(1 + p/\epsilon)(1 + 4\pi r^3 p/m)}{1 - 2Gm/r}, \quad (9)$$

$$\frac{dm}{dr} = 4\pi r^2 \epsilon, \quad (10)$$

being G the gravitational constant. Starting with a central mass density $\epsilon(r = 0) \equiv \epsilon_c$, one integrates out until the surface density equals the one of iron. This gives the stellar radius R and its gravitational mass $M = m(R)$. For the description of the NS crust, we have joined the hadronic EOS with the ones by Negele and Vautherin [13] in the medium-density regime, and the ones by Feynman-Metropolis-Teller [14] and Baym-Pethick-Sutherland [15] for the outer crust.

Due to the large number of configurations of hypernuclear matter that need to be calculated for a complete self-consistent determination of the EOS, a comparative study of several mass-radius relations based on independent choices of NN, NY, and YY potentials would be at the moment prohibitively time-consuming. We nevertheless think that the most important qualitative and even quantitative results are covered by the calculations that we carried out and explain in the following discussion of our numerical results.

We begin in Fig. 1 with the composition (particle fractions) and the EOS (pressure and energy density) of beta-stable

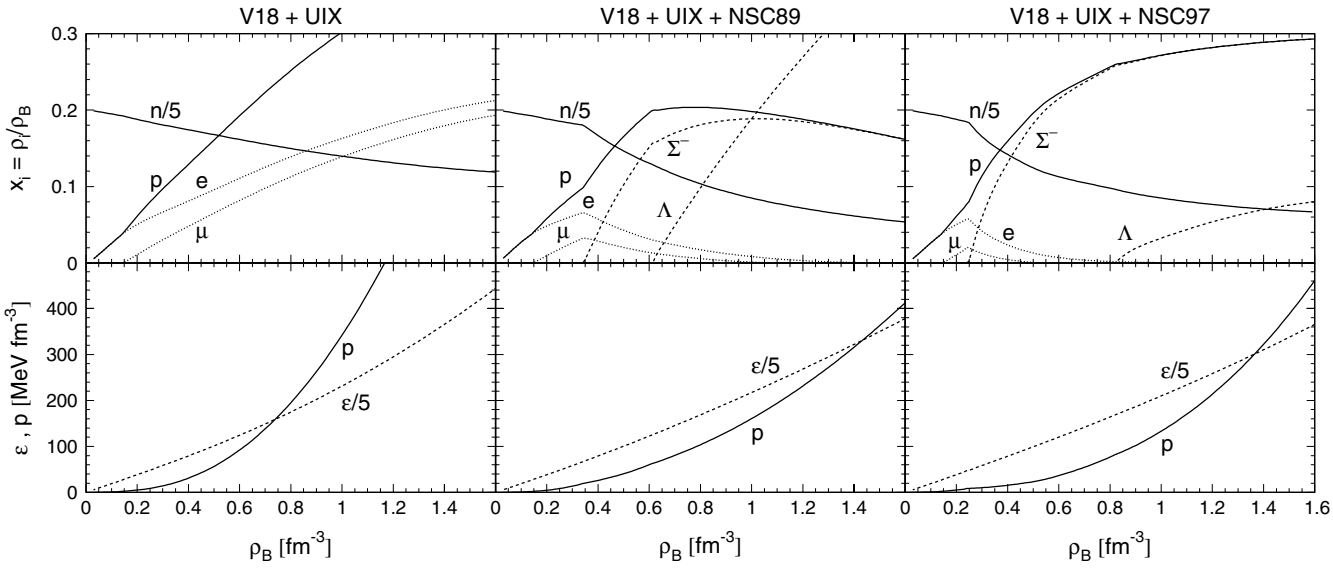

FIG. 1. Composition of β-stable matter (upper panels) and equation of state (lower panels) for different models.

matter obtained with three different EOS, namely the purely nucleonic V18+UIX and the hyperonic V18+UIX+NSC89 and V18+UIX+NSC97. One notes in the latter case the differences in the hyperon populations caused by the different characteristics of the *NY* and *YY* forces: The NSC97e potential contains quite attractive $n\Sigma^-$ and $\Sigma^-\Sigma^-$ forces, see, e.g., Ref. [4] for a detailed account of these aspects of this interaction model, leading to an earlier onset and a stronger population of Σ^- in the matter compared to the NSC89, while the Λ population remains much lower with the NSC97 due to repulsive $\Lambda\Lambda$ and $\Lambda\Sigma^-$ forces. Within our many-body approach, no hyperons other than Σ^- and Λ appear at densities below $\rho = 1.6$ fm^{-3}. These results differ from some present mean field calculations [16], where all kind of hyperons can appear at the densities considered here. Both hyperonic EOS are much softer (lower pressure and energy density) than the nucleonic one, which is essentially due to a decrease of the kinetic energy because the hyperons can be accomodated in lower momentum states and in addition have a large bare mass. The consequences of this softening are seen in the following results.

Figure 2 shows the mass-radius and mass-central density relations obtained with the different EOS. We first compare results [bold grey (online green) curves] obtained with three different purely nucleonic EOS, disallowing the appearance of hyperons, namely the V18+UIX, the V18+GLMM, and an EOS based on a variational calculation of nuclear matter [17], using the parametrization of Ref. [18], denoted APR in the following. The resulting maximum masses are relatively large, ranging from about 1.8 (V18+UIX) to 2.4 (V18+GLMM) solar masses.

In the next step [thin (red) curves] we include the hyperons and study the effect of changing only the nucleonic part of the EOS. In order to save substantial computation time this is done in an approximate manner, namely by performing the coupled BHF calculations described before with the complete set of NSC97 potentials, also including the *NN* components (the NSC97 *NN* potentials in this case are not of high precision [10] and also nucleonic TBF are not included), but maintaining only the hyperonic contribution ϵ_Y, Eq. (7), to the energy density from these calculations, while replacing the nucleonic part ϵ_N with one of the three different nucleonic EOS mentioned before. In this way the effect of the different *NN* potentials on the hyperons and also the rearrangement effects on the nucleons due to the presence of hyperons are neglected. However, this approximation is good enough for our purposes.

Doing so, one obtains a reduction of the maximum mass to about 1.5 $M_\odot$, but most importantly a strong reduction of the variation of the result with the nucleonic component of the EOS. The maximum masses obtained with the three EOS lie within a range of 0.15 $M_\odot$, compared to a range of 0.5 $M_\odot$ in the case without hyperons. This clearly emphasizes the important and well-known role of the hyperons as equalizing the effects of different nucleonic interactions: A stiffer nucleonic EOS causes an earlier onset and larger concentration of hyperons and therefore a stronger softening of the total EOS.

Finally, the bold black curves show our main and "best" results based on fully self-consistent calculations involving the coupled treatment of hyperons and nucleons as described above, with the Argonne V18+UIX *NN* and either the NSC89 or the NSC97 *NY* and *YY* potentials. The overall effect is a further reduction of the maximum mass by about 0.2 $M_\odot$, to 1.35 $M_\odot$ with the NSC97 and 1.31 $M_\odot$ with the NSC89 model. These values are quite similar in spite of the great differences of the composition of matter illustrated in Fig. 1.

We observe thus several compensation mechanisms, always leading to a soft EOS and keeping the maximum mass low: A stiffer nucleonic EOS will lead to an earlier onset of hyperons and thus enhanced softening due to their presence. Conversely, later onset of a certain hyperon species will favor the appearance of other species leading also to a softer EOS [24]. The resulting maximum mass is surprisingly insensitive to the purely nucleonic EOS and even to details of the *NY* and *YY* interactions. There remain, however, characteristic differences between the mass-radius relations that would

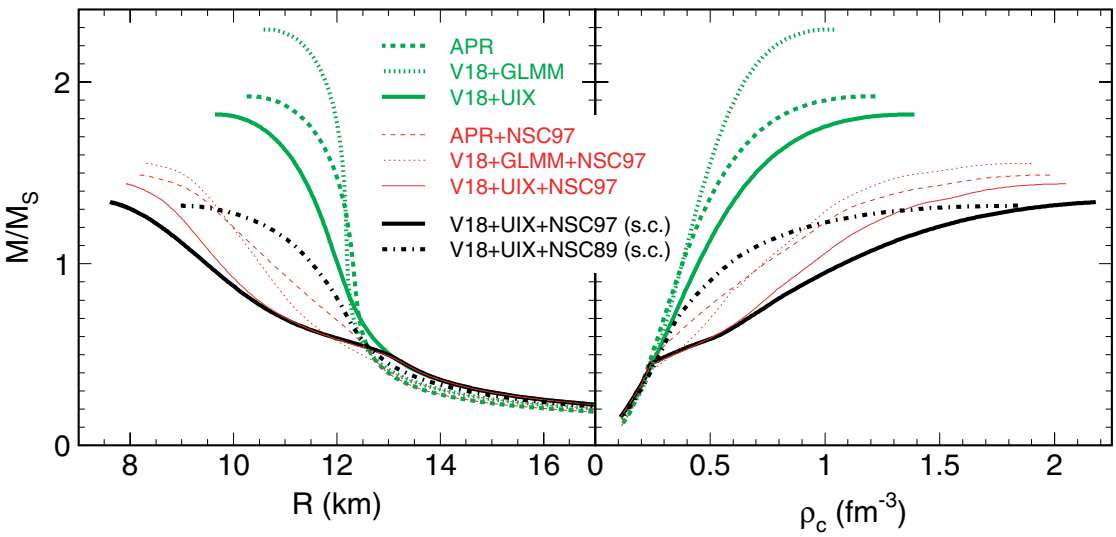

FIG. 2. (Color online) Mass-radius and mass-central density relations for different equations of state. Details are given in the text.

eventually allow one to determine the EOS from a combined M, R measurement, which is much awaited since a long time.

We have thus shown that a reliable microscopic EOS of high-density baryonic matter based on realistic *NN* and *NY* forces leads to very low masses of "neutron stars," even below the current observational limit of 1.44 $M_\odot$.

This feature has been demonstrated to be largely independent of the nucleonic part of the EOS due to a strong compensation mechanism caused by the appearance of hyperons. We have also used two completely different *NY* potentials (fitted to the same scattering data, however) which yield quite different internal compositions of the stars, but nevertheless the same maximum mass within 0.05 $M_\odot$.

Due to the complete lack of experimental and theoretical information, we have not included hyperonic TBF, but it seems difficult to imagine that these could strongly increase the maximum mass in view of various compensation mechanisms: Any delayed appearance and weaker concentration of a given species will favor the presence of the other baryons and restore a soft EOS.

Thus the only remaining possibility of increasing substantially the maximum mass appears to be the presence of non-baryonic, i.e., "quark" matter, in the star's interior. Indeed, our previous calculations using different effective quark matter EOS (bag model [19], NJL model [20], color dielectric model [21]) allow maximum masses of up to 1.8 $M_\odot$.

However, neutron star masses substantially above 2 $M_\odot$ seem to be out of reach even for these hybrid stars. The observational confirmation of such a heavy neutron star [23] would in our opinion indeed present a great challenge to our present theoretical understanding of high-density matter.

In the meantime it remains very important to construct improved *NY* and *YY* potentials and hyperonic TBF (constrained by future experimental data) in order to narrow even more the theoretical margin of uncertainty of the maximum mass of a baryonic star.

We would like to acknowledge valuable discussions with M. Baldo. This work is partially supported by the Grant No. FIS2005-03142 from MEC (Spain) and FEDER, and the Generalitat de Catalunya Project No. 2005SGR-00343.

[1] S. L. Shapiro and S. A. Teukolsky, *Black Holes, White Dwarfs and Neutron Stars* (Wiley, New York, 1983); N. K. Glendenning, *Compact Stars: Nuclear Physics, Particle Physics and General Relativity*, 2nd ed. (Springer, Berlin, 2000).

[2] H. Q. Song, M. Baldo, G. Giansiracusa, and U. Lombardo, Phys. Rev. Lett. **81**, 1584 (1998); M. Baldo, G. Giansiracusa, U. Lombardo, and H. Q. Song, Phys. Lett. **B473**, 1 (2000); M. Baldo, A. Fiasconaro, H. Q. Song, G. Giansiracusa, and U. Lombardo, Phys. Rev. C **65**, 017303 (2002).

[3] H.-J. Schulze, M. Baldo, U. Lombardo, J. Cugnon, and A. Lejeune, Phys. Rev. C **57**, 704 (1998); M. Baldo, G. F. Burgio, and H.-J. Schulze, *ibid.* **58**, 3688 (1998); **61**, 055801 (2000).

[4] I. Vidaña, A. Polls, A. Ramos, M. Hjorth-Jensen, and V. G. J. Stoks, Phys. Rev. C **61**, 025802 (2000).

[5] R. B. Wiringa, V. G. J. Stoks, and R. Schiavilla, Phys. Rev. C **51**, 38 (1995).

[6] B. S. Pudliner, V. R. Pandharipande, J. Carlson, S. C. Pieper, and R. B. Wiringa, Phys. Rev. C **56**, 1720 (1997); M. Baldo, I. Bombaci, and G. F. Burgio, Astron. Astrophys. **328**, 274 (1997); M. Baldo and L. S. Ferreira, Phys. Rev. C **59**, 682 (1999); X. R. Zhou, G. F. Burgio, U. Lombardo, H.-J. Schulze, and W. Zuo, *ibid.* **69**, 018801 (2004).

[7] P. Grangé, A. Lejeune, M. Martzolff, and J.-F. Mathiot, Phys. Rev. C **40**, 1040 (1989).

[8] W. Zuo, A. Lejeune, U. Lombardo, and J.-F. Mathiot, Nucl. Phys. **A706**, 418 (2002); Eur. Phys. J. A **14**, 469 (2002).

[9] P. M. M. Maessen, Th. A. Rijken, and J. J. de Swart, Phys. Rev. C **40**, 2226 (1989).

[10] V. G. J. Stoks and Th. A. Rijken, Phys. Rev. C **59**, 3009 (1999).

[11] Th. A. Rijken, V. G. J. Stoks, and Y. Yamamoto, Phys. Rev. C **59**, 21 (1999).

[12] J. Cugnon, A. Lejeune, and H.-J. Schulze, Phys. Rev. C **62**, 064308 (2000); I. Vidaña, A. Polls, A. Ramos, and H.-J. Schulze, *ibid.* **64**, 044301 (2001).

[13] J. W. Negele and D. Vautherin, Nucl. Phys. **A207**, 298 (1973).

[14] R. P. Feynman, N. Metropolis, and E. Teller, Phys. Rev. **75**, 1561 (1949).

[15] G. Baym, C. Pethick, and P. Sutherland, Astrophys. J. **170**, 299 (1971).

[16] R. Knorren, M. Prakash, and P. J. Ellis, Phys. Rev. C **52**, 3470 (1995); J. Schaffner and I. N. Mishustin, *ibid.* **53**, 1416 (1996); M. Prakash, I. Bombaci, M. Prakash, P. J. Ellis, J. M. Lattimer, and R. Knorren, Phys. Rep. **280**, 1 (1997).

[17] A. Akmal, V. R. Pandharipande, and D. G. Ravenhall, Phys. Rev. C **58**, 1804 (1998).

[18] H. Heiselberg and M. Hjorth-Jensen, Phys. Rep. **328**, 237 (2000).

[19] G. F. Burgio, M. Baldo, P. K. Sahu, and H.-J. Schulze, Phys. Rev. C **66**, 025802 (2002).

[20] M. Baldo, M. Buballa, G. F. Burgio, F. Neumann, M. Oertel, and H.-J. Schulze, Phys. Lett. **B562**, 153 (2003).

[21] C. Maieron, M. Baldo, G. F. Burgio, and H.-J. Schulze, Phys. Rev. D **70**, 043010 (2004).

[22] H. Noumi *et al.*, Phys. Rev. Lett. **89**, 072301 (2002); P. K. Saha *et al.*, Phys. Rev. C **70**, 044613 (2004).

[23] D. J. Nice, E. M. Splaver, I. H. Stairs, O. Loehmer, A. Jessner, M. Kramer, and J. M. Cordes, astro-ph/0508050.

[24] This compensation mechanism would also hold in case the Σ^- felt a repulsive potential as some recent experiments seem to suggest [22].